



Cite this: *Org. Biomol. Chem.*, 2015, **13**, 11704

Design, synthesis and DNA interactions of a chimera between a platinum complex and an IHF mimicking peptide†

Harita Rao,^a Mariana S. Damian,^{a,b} Alak Alshiekh,^b Sofi K. C. Elmroth^b and Ulf Diederichsen^{*a}

Conjugation of metal complexes with peptide scaffolds possessing high DNA binding affinity has shown to modulate their biological activities and to enhance their interaction with DNA. In this work, a platinum complex/peptide chimera was synthesized based on a model of the Integration Host Factor (IHF), an architectural protein possessing sequence specific DNA binding and bending abilities through its interaction with a minor groove. The model peptide consists of a cyclic unit resembling the minor groove binding subdomain of IHF, a positively charged lysine dendrimer for electrostatic interactions with the DNA phosphate backbone and a flexible glycine linker tethering the two units. A norvaline derived artificial amino acid was designed to contain a dimethylethylenediamine as a bidentate platinum chelating unit, and introduced into the IHF mimicking peptides. The interaction of the chimeric peptides with various DNA sequences was studied by utilizing the following experiments: thermal melting studies, agarose gel electrophoresis for plasmid DNA unwinding experiments, and native and denaturing gel electrophoresis to visualize non-covalent and covalent peptide–DNA adducts, respectively. By incorporation of the platinum metal center within the model peptide mimicking IHF we have attempted to improve its specificity and DNA targeting ability, particularly towards those sequences containing adjacent guanine residues.

Received 10th September 2015,
Accepted 6th October 2015

DOI: 10.1039/c5ob01885d

www.rsc.org/obc

Introduction

One of the very well established mechanisms by which cis-platin and related chemotherapeutics manifest their cytotoxic effects is by forming covalent crosslinks mostly with adjacent guanine residues of nuclear DNA.^{1–5} The resulting kinked structure of DNA is stabilized by the binding of the High Mobility Group (HMG) domain proteins which block the cellular repair mechanism.^{6–8} Subsequently, inhibition of essential cellular processes such as replication and transcription lead ultimately to induction of apoptosis.^{9–12} Apart from nuclear DNA, the platinum drugs can potentially target various other cellular components such as cytosolic proteins and can in parallel trigger biochemical pathways resulting in cytotoxicity.^{13–16} However, their side reactions with certain cytoskeletal nucleophiles such as thiols, phospholipids, microfilaments or RNA either deactivate the drugs or lead to several undesired secondary effects.^{17–20} These include toxic effects such as neuro-

toxicity, nephrotoxicity, ototoxicity, emetogenesis^{21–24} as well as onset of resistance in cancer cells.^{25,26}

Drug candidates with enhanced targeting of nuclear DNA in comparison with other cellular components can be considered a promising approach to foster the clinical applicability of platinum complexes. Conjugation of metal complexes with suitable carrier molecules having intrinsic binding affinity and recognition properties for nucleic acid sequences has proven to be an efficient delivery system for specifically targeting DNA.^{27–30} Thus, implementing peptide backbones as biological carriers offers a plethora of advantages due to their high bioavailability and cell penetrating, target directing and recognition properties.^{31–33} In our previous work, platinum complex/peptide chimera consisting of positive charged lysine residues showed enhanced binding to the polyanionic DNA.³⁴ This approach to develop chimeric platinum complexes offers the possibility to have a unique DNA interaction mode that is distinct from the metal complex alone.³⁵ We extended this work towards a more specific DNA targeting, by designing a platinum complex/peptide chimera using model peptides mimicking the IHF, a protein known for its ability to bind to the DNA minor groove with a high degree of sequence specificity.³⁶

IHF is a chromatin architectural protein belonging to the family of bacterial type II DNA binding proteins.^{36,37} It plays a

^aInstitut für Organische und Biomolekulare Chemie, Georg-August-Universität Göttingen, Tammannstrasse 2, 37077 Göttingen, Germany.

E-mail: udieder@gwdg.de

^bBiokemi, Kemicentrum, Lund Universitet, P. O. Box 124, 22100, Lund, Sweden

† Electronic supplementary information (ESI) available. See DOI: 10.1039/c5ob01885d



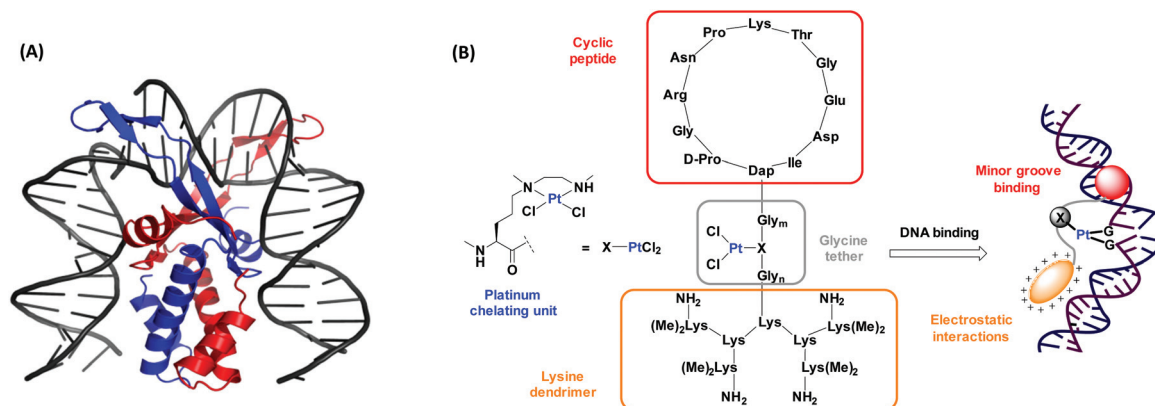


Fig. 1 (A) The cocrystal structure of IHF bound to a 35 bp dsDNA fragment consisting of the H' site of phage λ . The α -subunit is shown in red and the β -subunit in blue. Image reproduced using PyMOL (PDB entry: 1IHF).⁴⁰ (B) Our model of the platinum complex/peptide chimera mimicking the α -subunit of IHF for targeting DNA by minor groove binding (through the cyclic peptide shown in red) and by electrostatic interactions with the negatively charged DNA (through the lysine dendrimer shown in orange). The IHF mimicking units are attached through a glycine linker wherein, the platinum chelating unit (X) is flexibly inserted to provide a second DNA recognition center.

crucial role in processes demanding higher order structural organization of DNA such as replication, transcription and site specific recombination.^{38,39} The IHF-DNA cocrystal (Fig. 1A),⁴⁰ consists of two intertwined subunits, the α - and the β -subunit, forming a compact body from which two long flexible ribbon like arms protrude and wrap around the DNA minor groove. Intercalation of a proline residue located at the tip of each arm between the base pairs, disrupts the stacking interactions and leads to the formation of two sharp kinks of $>160^\circ$ in the DNA structure. Combination of the IHF mimicking model peptide with a platinum chelating unit is expected to have a synergistic effect with respect to the interaction with DNA (Fig. 1B). Here we present a synthetic route to access the IHF mimicking platinum complex/peptide chimera for achieving enhanced DNA recognition properties, and performed preliminary DNA interaction studies.

Results and discussion

The design of the IHF mimicking peptides is based on the model peptide **IHF-1** (Fig. 2) as reported earlier.^{41,42} It has a closer resemblance to the α -subunit of IHF mainly due to its contribution to sequence specific DNA recognition within the minor groove.⁴⁰ However, for the model peptide **IHF-1** only a modest DNA bending effect was observed based on FRET measurements of respectively labeled DNAs.⁴² The basic structure of the IHF mimicking peptides can be divided into three parts, wherein each part contributes to different kinds of interactions with DNA (Fig. 1B). Firstly, a cyclic peptide unit resembles the minor groove binding loop of the IHF α -subunit and consists of the amino acid residues around the intercalating proline. Secondly, a lysine dendrimer mimics the positively charged body of IHF in order to compensate for electrostatic interactions with the negatively charged DNA phosphate backbone. Thirdly, a glycine linker not only tethers the two main

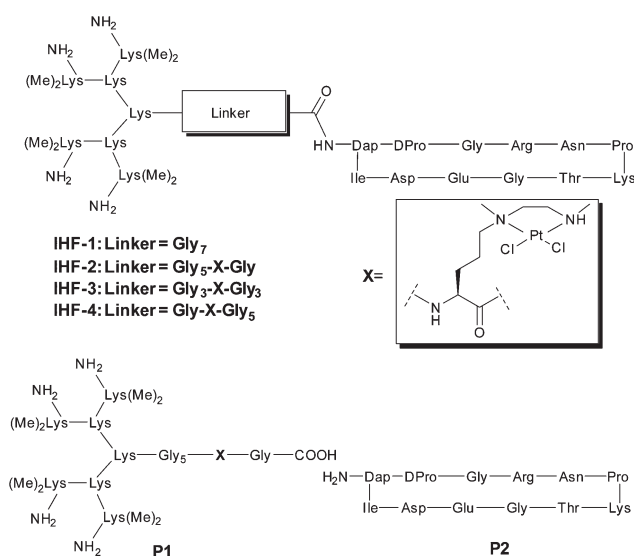


Fig. 2 Various IHF mimicking peptides used in this study: **IHF-1** is the unplatinated peptide, the mimics **IHF-2**, **IHF-3** and **IHF-4** contain a platinum chelating unit at different positions within the glycine linker, **P1** is the platinated dendrimeric peptide and **P2** is the cyclic peptide mimicking the minor groove intercalating unit.

peptide units but also has a functional role by containing a norvaline derived platinum chelating artificial amino acid. The platinated IHF mimics were prepared by placing the platinum metal center at flexible positions within the glycine linker: in close proximity to the cyclic unit (**IHF-2**), in the middle (**IHF-3**), and near the dendrimeric unit (**IHF-4**), respectively. The DNA interaction of the platinated mimics **IHF-2/3/4** was compared to that of the platinated dendrimeric peptide **P1**, cyclic peptide **P2** and the unplatinated IHF mimic **IHF-1** (Fig. 2). Irrespective of the position of the platinum center within the glycine linker all three mimics **IHF-2/3/4** showed



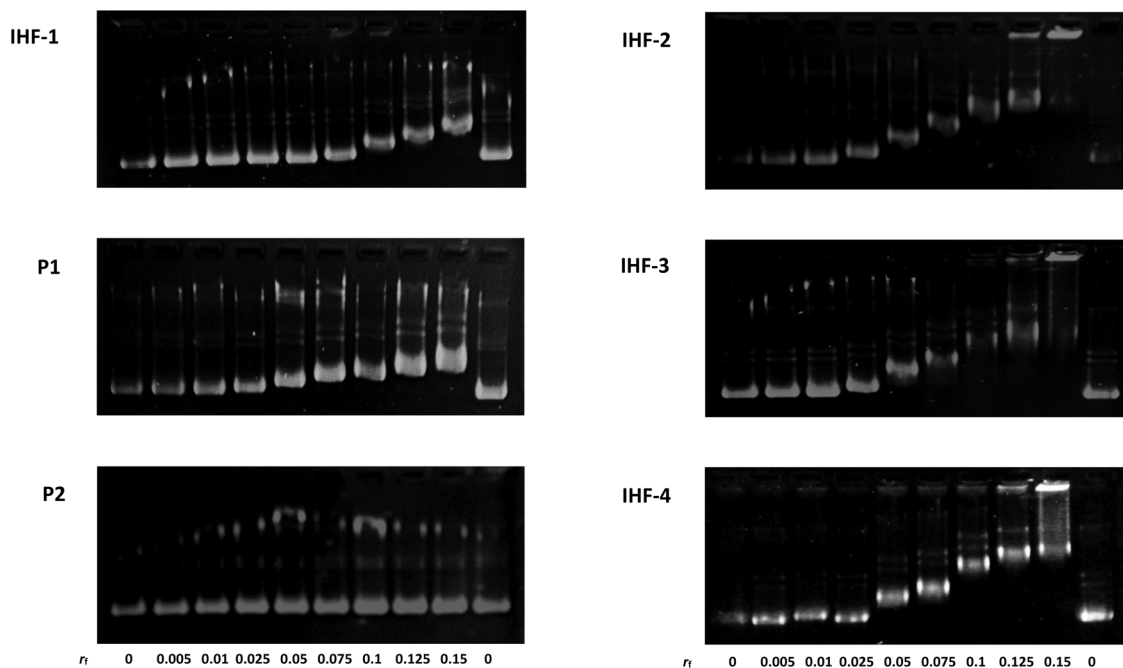


Fig. 3 Agarose gel electrophoresis to study the interactions of the IHF mimicking peptides **IHF-1/2/3/4**, the platinated lysine dendrimer **P1** and the cyclic peptide **P2** with pUC18 plasmid DNA (incubation time for 2 h at 37 °C, with r_f varying from 0 to 0.15, 10 mM $\text{Na}_2\text{HPO}_4/\text{NaH}_2\text{PO}_4$, pH 5.8, $[\text{pUC18}] = 0.2$ mM nucleobases).

the platinum unit, known to distort DNA's structure due to a local unwinding of the duplex.⁴⁵ Gel mobility shift assays utilizing native agarose gel electrophoresis were performed in order to study the conformational changes induced in the circular plasmid DNA upon interaction with various synthetic peptides (Fig. 3). The supercoiled form of the plasmid has a more compact structure and hence migrates faster in comparison with the relaxed form. Unwinding of the plasmid DNA affects the degree of supercoiling influencing its migration pattern on the gel; an increasing amount of platinated DNA is expected to be visualized by appearance of a slower migrating band.⁴⁶ The ratio of the nucleotide (C_{DNA}) to the peptide derivative (C_{peptide}) concentration ($r_f = C_{\text{peptide}}/C_{\text{DNA}}$) was varied in the range of 0–0.15 and the peptides were incubated for 2 h at 37 °C in 10 mM phosphate buffer, pH = 5.8.

In this study the interaction of the IHF mimicking peptides **IHF-1/2/3/4**, the platinated lysine dendrimer **P1**, and the non-platinated cyclic peptide **P2** was tested with the negatively supercoiled pUC18 plasmid. The platinated IHF mimics **IHF-2/3/4** interact with DNA *via* both covalent as well as non-covalent interactions whereas **IHF-1** can interact with DNA only through non-covalent interactions. All three platinated mimics **IHF-2/3/4** led to the formation of slower migrating bands already at a lower r_f value of 0.05 compared to the unplatinated IHF mimic **IHF-1** which only had an effect on the plasmid DNA migration pattern at an r_f around 0.1. This is a first clue that the presence of the platinum chelating unit in the IHF mimics results in enhanced DNA binding and unwinding.

The platinated dendrimeric peptide **P1** induces a shift starting at an r_f of 0.075, whereas the cyclic peptide **P2** does not show an efficient gel mobility shift in the plasmid DNA migration pattern. The cyclic peptide **P2** had no influence on the migration properties of the supercoiled plasmid due to lack of electrostatic forces for having sufficient interaction with the negatively charged DNA, unless it is connected to the positively charged body of the dendrimeric peptide. The effect is emphasized when comparing **P2** with **IHF-1**. This is an indication that the cyclic peptide **P2** does not affect plasmid unwinding and that only incorporation within the IHF mimics brings it in close proximity to the interaction center, facilitating DNA binding.

Moreover, on comparing the platinated compound **P1** with its platinum-IHF analogues, **IHF-2/3/4**, it is obvious that the platinated IHF mimics induce a higher DNA unwinding compared to the platinated lysine dendrimer. Hence, the electrostatic interactions of the dendrimeric peptide with the plasmid DNA solely are not enough to distort its structure, but it influences the effect of the whole IHF mimic. Therefore, the connection of the two IHF mimicking peptide units and platination are necessary to have an optimum interaction, and furthermore, structural distortion of DNA.

Binding studies with the IHF consensus sequence

Native and denaturing polyacrylamide gel electrophoresis were utilized to investigate the interactions of the IHF mimicking peptides with 34-mer DNA duplexes consisting of the IHF con-



sensus sequence. Native gels allow visualization of the binding events resulting from both covalent and non-covalent interactions whereas denaturing gels assist in specifically visualizing covalent linkages between the peptide and the DNA. The following two DNA sequences were applied in this study: (3'-ATTTTTTCGTAACGGATAGTTAAACAACGTTGCT-5') and (3'-ATTTTTTCGTAACGAATAGTTAAACAACGTTGCT-5'). In the former sequence, adjacent guanine residues (GG site) were introduced due to their greater tendency for platination. The oligomers consisted of a fluorescent 6-carboxyfluorescein label at the 5' end for visualization and were annealed with their complementary DNA to give duplexes **D1** and **D2**, respectively. The peptides were incubated with the duplexes for 17 h at 37 °C in 10 mM Na₂HPO₄/NaH₂PO₄, 100 mM NaClO₄, pH = 5.8 prior to electrophoresis. Since in polyacrylamide gels, larger molecules tend to have a slower migration pattern,^{41,47–49} the binding of the peptide to the DNA was monitored by appearance of a slower migrating band compared to the unbound DNA.

In both native and denaturing gels, the platinated IHF mimics exhibit stronger binding to duplex **D1** containing a GG site (Fig. 4a and b) compared to duplex **D2** without a GG site (Fig. 4c and d). On the contrary, the unplatinated peptide **IHF-1** (lane 2) does not bind to either of the two sequences indicating a crucial role of the platinum unit in enhanced DNA interaction. Changing the position of the GG site within a given DNA sequence doesn't seem to influence the binding of the platinum-IHF mimics (see ESI Fig. S1†). This reveals their lack of sequence specificity for targeting a particular DNA.

The interaction of the IHF mimics with duplex **D1** containing the GG site was studied in detail both in the absence (lanes 1–6) and in the presence (lanes 7–11) of cisplatin (Fig. 4a and b). All platinated peptides induced a shift in the migration pattern of DNA (lanes 3–6 and lanes 7–11). In the absence of cisplatin (lanes 3–6), the first product band with the highest intensity corresponds to the mono-peptide–DNA adduct, whereas the other less intense bands with further gel shifts correspond to various higher order adducts. The native gel reveals (Fig. 4a), a comparable amount of peptide–DNA adduct formation with platinum-IHF mimics, **IHF-2/3/4** in the presence and absence of cisplatin (lanes 3–5 & 7–10, 50% average yield). The denaturing gel indicates (Fig. 4b) a vast difference in the formation of the peptide–DNA adduct with **IHF-2/3/4** in the absence of cisplatin (lanes 3–5, 40% average yield) when compared to that in the presence of five times excess of cisplatin (lanes 7–10, 15% average yield). These differences point towards the ability of platinum-IHF mimics to non-covalently interact with the cisplatin modified DNA, which can still have a synergistic effect on DNA interactions. Additionally, covalent binding of platinum-IHF mimics to the GG site containing duplex **D1** even in the presence of five times excess of cisplatin clearly indicates a competition between the two for the same binding site.

The native gel indicates (Fig. 4a) the platinated dendrimeric peptide **P1** led to nearly complete disappearance of the unbound DNA band due to the formation of multiple adducts, most of which were below the level of detection. Moreover, the denaturing gel displays (Fig. 4b) a much weaker covalent

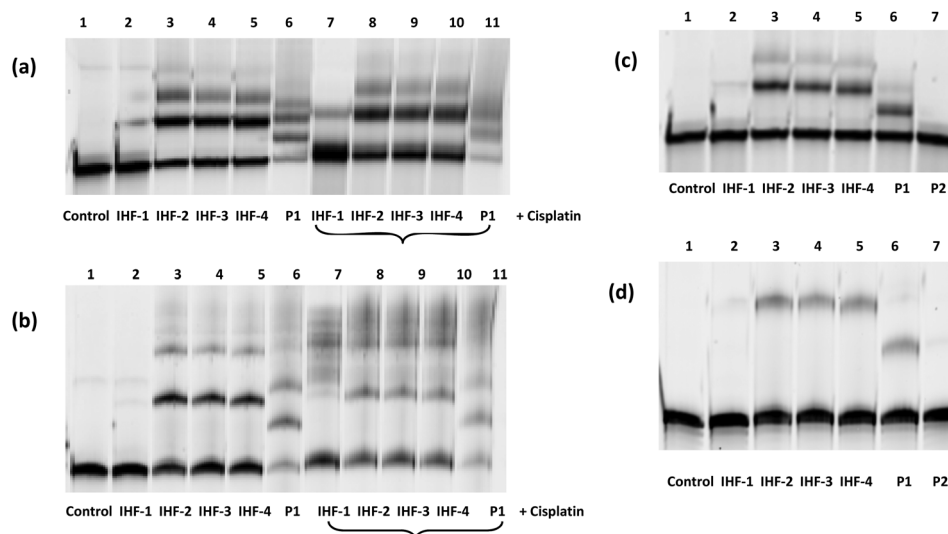


Fig. 4 Polyacrylamide gel electrophoresis assay to study the interactions of the IHF mimicking peptides with the 34 mer DNA duplex **D1**, consisting of a GG site and the duplex **D2**, excluding the GG site. The samples were incubated for 17 h at 37 °C in 10 mM Na₂HPO₄/NaH₂PO₄, 100 mM NaClO₄, pH 5.8. (a) and (b) Lanes 1–11 contain 0.5 μM DNA duplex **D1**. Lanes 2, 3, 4, 5, 6 contain 10 μM of **IHF-1**, **IHF-2**, **IHF-3**, **IHF-4**, **P1** respectively. Lanes 7, 8, 9, 10 and 11 contain an additional 50 μM cisplatin to **IHF-1**, **IHF-2**, **IHF-3**, **IHF-4**, **P1** respectively. (c) and (d) Lanes 1–7 contain 0.5 μM DNA duplex **D2**. Lanes 2, 3, 4, 5, 6, 7 contain 10 μM of **IHF-1**, **IHF-2**, **IHF-3**, **IHF-4**, **P1**, **P2** respectively. (a) and (c) Performed under non-denaturing conditions (20% PAA, 1x TBE). (b) and (d) Performed under denaturing conditions (20% PAA, 7 M urea, 1x TBE).



binding of **P1** (lane 6, 20%; lane 11, 10%) both in the absence and presence of cisplatin compared to **IHF-2/3/4**. These results further validate the design of the IHF mimicking platinum complex/peptide chimera which include the minor groove binding cyclic peptide, a positively charged lysine dendrimer for electrostatic interactions and a platinum unit for covalent linkage with DNA.

Thermal melting analysis

The effects of the IHF mimicking peptides on the thermal stability of the 34-mer duplex **D1** containing a GG-site within the IHF consensus sequence was analyzed by monitoring temperature dependent UV absorbance (Fig. 5). The observed melting profile of the DNA duplex is a net result of its interactions with the peptidic scaffold and the platinum unit. The platinum complexes distort the structure of DNA by forming covalent crosslinks and depending on the type of crosslinking they either enhance or reduce the stability of the duplex.^{50,51} On the other hand, binding of the positively charged DNA ligands apparently enhances the duplex stability.⁵² Prior to measurement the peptides were pre-incubated with the duplex for 17 h at 37 °C. Thermal denaturation and subsequent renaturation processes were studied by heating from 20 to 95 °C and cooling from 95 to 10 °C, respectively. The melting temperatures (T_m) for each cycle were obtained by calculating the maxima of the first derivative of the heating and the cooling curves (Table 1).

In line with the reversibility of melting curves, the denaturation and renaturation cycles were nearly superimposable for the duplex **D1** (1 μ M, 10 mM $\text{Na}_2\text{HPO}_4/\text{NaH}_2\text{PO}_4$, pH = 5.8) in the absence of peptides as well as in the presence of unplatinated peptides, **IHF-1** and cyclic peptide **P2**. While the unplatinated IHF mimic **IHF-1** led to a sharp increase in melting temperature ($\Delta T_m \geq 12$ °C) of duplex **D1**, the cyclic peptide **P2** had a mild stabilization effect ($\Delta T_m = 1$ °C). This indicates that

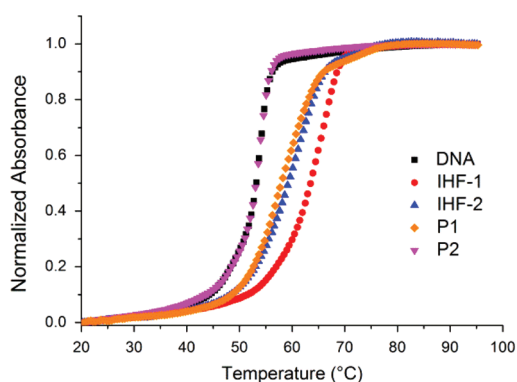


Fig. 5 UV melting profile of duplex **D1** studied after pre-incubation with the IHF mimicking peptides **IHF-1/2**, **P1**, **P2** as well as DNA alone for 17 h at 37 °C (1 μ M of DNA with 5 μ M of peptides) in 10 mM $\text{Na}_2\text{HPO}_4/\text{NaH}_2\text{PO}_4$, pH = 5.8. The melting profiles of **IHF-2/3/4** were found to be similar and the profile for only **IHF-2** has been used for representation.

Table 1 Summary of melting temperatures (T_m) of a GG-site containing 34-mer duplex **D1** for two subsequent cycles, heating from 20 to 95 °C (denaturation) and cooling from 95 to 10 °C (renaturation)

Peptide ^a	Denaturation (20–95) °C		Renaturation (95–10) °C	
	T_m (°C)	ΔT_m^b (°C)	T_m (°C)	ΔT_m^b (°C)
Control	53.6 ± 0.5	—	52.7 ± 0.1	—
IHF-1	65.6 ± 0.1	+12.0	66.0 ± 0.1	+13.3
IHF-2	61.5 ± 1.5	+7.9	50.2 ± 0.9	−2.5
IHF-3	62.1 ± 0.9	+8.5	50.0 ± 0.1	−2.7
IHF-4	59.6 ± 0.6	+6.0	50.6 ± 0.6	−2.1
P1	57.9 ± 0.3	+4.3	51.1 ± 0.7	−1.6
P2	54.1 ± 0.1	+0.5	53.9 ± 0.1	+1.2

^a The peptides were pre-incubated with the duplex **D1** for 17 h at 37 °C in 10 mM phosphate buffer, pH = 5.8 where the concentration of the DNA was 1 μ M and the concentration of the peptide was 5 μ M. ^b ΔT_m represents T_m (in the presence of peptide) – T_m (control DNA) for the heating and the cooling curve, respectively.

while **IHF-1** stabilizes the duplex by electrostatic interactions with its negatively charged phosphate backbone, the cyclic peptide **P2** can only interact weakly with the duplex in the absence of the positively charged lysine dendrimer. The platinated mimics **IHF-2/3/4** and the dendrimeric peptide **P1**, however, did not exhibit reversibility of the melting profile for the heating and cooling cycle. In the heating cycle, though less in comparison to the unplatinated mimic **IHF-1**, all the platinated IHF mimics ($\Delta T_m = 6$ –8 °C) and the dendrimeric peptide **P1** ($\Delta T_m = 4$ °C) indicate a net stabilizing effect on the duplex. At elevated temperatures single stranded DNA obtained after denaturation of the duplex is readily accessible for reaction with the platinum complex/chimera, triggering the formation of a covalent linkage between the platinated peptides and DNA. This hinders the renaturation process of the duplex and as a result, a net decrease in the melting temperature is observed.

Experimental section

General

All purchased chemical reagents were of analytical grade and were utilized as received from the supplier. All solvents were of the highest commercial grade available. All the amino acid derivatives, coupling reagents and resins utilized in solid peptide synthesis were purchased from NovaBiochem (Darmstadt, Germany), GL Biochem (Shanghai, China), ABCR (Karlsruhe, Germany), Bachem (Bubendorf, Switzerland), IRIS Biotech (Marktredwitz, Germany), Merck (Darmstadt, Germany) and VWR (Darmstadt, Germany). All other chemical reagents were obtained from Carl Roth GmbH (Karlsruhe, Germany), Fisher Scientific GmbH (Nidderau, Germany), Alfa Aesar (Karlsruhe, Germany), Bachem (Bubendorf, Switzerland), TCI (Eschborn, Germany), NovaBiochem (Darmstadt, Germany), Sigma Aldrich (Taufkirchen, Germany) and Acros Organic (Geel, Belgium). DNA oligomers used for binding experiments were supplied by Biomers (Ulm, Germany). Ultra-



pure water was obtained utilizing the water purification system "Simplicity" (Millipore, Bedford, UK). The artificial amino acid residues *N*-*tert*-butoxycarbonyl- δ -bromo-norvaline benzyl ester and $N\alpha$ -Boc- $N\epsilon$, $N\epsilon$ -dimethyl-*L*-lysine were prepared by following literature known procedures.^{43,53} Glassware utilized for performing reactions under an argon atmosphere were flame dried prior to usage. Thin layer chromatography (TLC) was performed using Merck aluminium backed plates coated with silica gel F254. Purification by flash chromatography was performed using Merck silica gel 60. The compounds were visualized under UV light or by staining with ninhydrin solution followed by charring.

¹H and ¹³C NMR spectra were recorded on a Varian Unity 300 or Varian Inova 500 spectrometer. The chemical shifts (δ) reported in parts per million (ppm) denote a downfield shift relative to trimethylsilane (TMS), taken as the internal standard. Signal multiplicities were abbreviated as: s, singlet; d, doublet; t, triplet; q, quartet; m, multiplet; b, broad. The coupling constants (*J*) were reported in hertz (Hz). ESI mass spectra were measured on a Finnigan instrument (type LCQ or TSQ 7000) and high-resolution mass spectra were measured on Bruker spectrometers (types Apex-Q IV 7 T, microTOF API). Fmoc solid phase peptide synthesis was performed manually utilizing standard protocol and coupling reagents 1-[bis(dimethylamino)methylene]-1*H*-1,2,3-triazolo[4,5-*b*] pyridinium 3-oxid hexafluorophosphate (HATU) and 1-hydroxy azabenzotriazole (HOAt). HPLC was carried out on Amersham Pharmacia Biotech systems (Äkta basic, Pump type P-900, variable wavelength detector, GE Healthcare, London, UK). A linear gradient of A (0.1% TFA in H₂O) to B (0.1% TFA in MeCN/H₂O, 8/2, (v/v)) or to B' (0.1% TFA in MeCN/H₂O, 9/1, (v/v)) was applied and the UV absorption was monitored at 215 nm. Peptides were analyzed and purified utilizing a Macherey-Nagel Nucleodur 100 column, RP-C18, 250 × 21.0 mm, 5 μ m, with a flow rate of 10 mL min⁻¹ or a Macherey-Nagel Nucleodur 100 column, RP-C18, 250 × 21.0 mm, 5 μ m, with a flow rate of 3 mL min⁻¹. The concentration of the oligonucleotides was determined by utilizing the extinction co-efficient at 260 nm and measuring absorbance using a Nanodrop ND-2000c spectrometer.

***N*-Allyloxycarbonyl-*N,N*-dimethylethylenediamine (2).** Allyl phenyl carbonate (4.82 mL, 30 mmol, 1 eq.) was added dropwise to a solution of *N,N*-dimethylethylenediamine **1** (6.54 mL, 60 mmol, 1 eq.) in EtOH (200 mL). After stirring the reaction mixture overnight at room temperature the solvent was removed under vacuum and the residue was dissolved in water (200 mL). The pH of the solution was adjusted to ~3 by adding 1 M HCl and the aqueous phase was extracted with DCM (4 × 200 mL). Thereafter, the pH of the mixture was made strongly alkaline (~13) with the addition of 1 M NaOH. The organic phase obtained from earlier extractions was discarded and the basic aqueous solution was again extracted with DCM (4 × 200 mL). The combined organic phase was washed with 2 M NaOH (3 × 200 mL) and dried over sodium sulphate. The solvent was removed under reduced pressure yielding the product *N*-allyloxycarbonyl-*N,N*-dimethyl-

ethylenediamine **2** (6.4 g, 37.2 mmol, 62%) as a colorless oil. ¹H-NMR (300 MHz, CDCl₃): δ (ppm) = 5.94–5.81 (m, 1-H, CH=CH₂), 5.28–5.12 (m, 2-H, CH=CH₂), 4.55–4.50 (m, 2-H, -OCH₂), 3.35 (t, ³J_{H-H} = 6.6 Hz, 2-H, N-CH₂), 2.90 (s, 3-H, N-CH₃), 2.70 (t, ³J_{H-H} = 6.6 Hz, 2-H, NH-CH₂), 2.39 (s, 3-H, NH-CH₃), 1.36 (s_{br}, 1-H, NH). ¹³C-NMR (125 MHz, CDCl₃): δ (ppm) = 156.1 (C=O), 133.0 (-CH=CH₂), 117.1 (-CH=CH₂), 66.0 (O-CH₂), 49.7 (NHCH₂), 48.6 (NCH₂), 36.4 (NHCH₃), 35.2 (NCH₃). MS (ESI): *m/z* = 173.1 [M + H]⁺, 195.1 [M + Na]⁺, 345.2 [2M + H]⁺, 367.2 [2M + Na]⁺. HRMS (ESI) = calculated for [C₈H₁₇N₂O₂]⁺ ([M + H]⁺) = 173.1285, found = 173.1286.

(*S*)-*N*-(*tert*-Butoxycarbonyl)- δ -(*N*-(allyloxycarbonyl)-*N,N'*-dimethylethylenediamino)norvaline benzyl ester (4). To a solution of *N*-allyloxycarbonyl-*N,N'*-dimethylethylenediamine **2** (4.01 g, 23.31 mmol, 3 eq.) in dry DMF (40 mL), DIEA (4 mL, 23.31 mmol, 3 eq.) was added under an argon atmosphere at room temperature. Thereafter, (*S*)-*N*-*tert*-butoxycarbonyl- δ -bromo-norvaline benzyl ester **3** (3 g, 7.77 mmol, 1 eq.) dissolved in dry DMF (35 mL) was added dropwise to this mixture. The reaction was allowed to stir for 48 h at room temperature and the solvent was removed under reduced pressure. The residue was dissolved in EtOAc and the organic layer was washed with water, dried over sodium sulphate and concentrated under vacuum. Purification by column chromatography [eluent: pentane/EtOAc, 1/1 (v/v) → EtOAc (100%)] yielded **4** as a colorless oil (3 g, 6.29 mmol, 81%). TLC [EtOAc/MeOH, 9/1 (v/v)]: *R*_f = 0.53. ¹H-NMR (300 MHz, DMSO-*d*₆): δ (ppm) = 7.40–7.30 (m, 5-H, Ar-H), 7.28 (d, ³J_{H-H} = 7.5 Hz, 1-H, NH), 5.97–5.84 (m, 1-H, CH=CH₂), 5.30–5.05 (m, 4-H, CH=CH₂, CH₂-Ph), 4.49 (dt, 2-H, ⁴J_{H-H} = 1.5 Hz, ³J_{H-H} = 5.4 Hz, CH₂-Alloc), 4.10–3.97 (m, 1-H, α -CH), 3.27 (t, ³J_{H-H} = 6.9 Hz, 2-H, CO-NCH₂), 2.83 (s, 3-H, CO-NCH₃), 2.39 (t, ³J_{H-H} = 6.75 Hz, 2-H, N-CH₂), 2.27 (t, ³J_{H-H} = 6.9 Hz, 2-H, δ -CH₂), 2.12 (s, 3-H, NCH₃), 1.72–1.55 (m, 2-H, β -CH₂), 1.46–1.40 (m, 2-H, γ -CH₂), 1.38 (s, 8-H, ^tBoc-CH₃), 1.29 (s, 1-H, ^tBoc-CH₃, rotamer). ¹³C-NMR (125 MHz, DMSO-*d*₆): δ (ppm) = 172.4 (CO-OBn), 155.5 (CO-Boc), 155.1 (CO-Alloc), 136.0 (Ph_{ipso}), 133.5 (-CH₂-CH=CH₂), 128.3, 127.9, 127.7 (Ph), 116.6 (-CH₂-CH=CH₂), 78.1 [C(CH₃)₃], 65.6 (CH₂-Ph), 64.9 (-CH₂-CH=CH₂), 56.5 (δ -CH₂), 54.4 (NCH₂), 53.5 (α -CH), 46.1 (CO-NH₂), 41.6 (NCH₃), 33.9 (CO-NCH₃), 28.4 (β -CH₂), 28.1 [C(CH₃)₃], 23.0 (γ -CH₂). MS (ESI): *m/z* = 478.3 [M + H]⁺, 476.3 [M - H]⁻. HRMS (ESI) = calculated for [C₂₅H₄₀N₃O₆]⁺ ([M + H]⁺) = 478.2912, found = 478.2917.

(*S*)-*N*-((9*H*-Fluoren-9-yl)methoxy)carbonyl)- δ -(*N*-(allyloxycarbonyl)-*N,N'*-dimethylethylenediamino)norvaline benzyl ester (5). (*S*)-*N*-(*tert*-Butoxycarbonyl)- δ -(*N*-(allyloxycarbonyl)-*N,N'*-dimethylethylenediamino)pentanoic acid benzyl ester **4** (1.8 g, 3.77 mmol, 1 eq.) was dissolved in dioxane (16.5 mL) followed by addition of water (11 mL) and 1 M aq. NaOH (5.5 mL). The mixture was stirred for 6 h at room temperature followed by neutralization with 1 M HCl (5.5 mL), concentration under vacuum and lyophilization. The obtained residue was dissolved in TFA/H₂O (95/5 (v/v), 30 mL) at 0 °C and stirred for an additional 15 min at 0 °C. After an additional stirring for 6 h at room temperature TFA was removed under vacuum, the



aqueous phase was co-evaporated with 1 N HCl (3 × 15 mL) and the mixture was lyophilized. The residue obtained was dissolved in 10% Na₂CO₃ (25 mL) and Fmoc-OSu (1.53 g, 4.53 mmol, 1.2 eq.) solubilized in dioxane (16 mL) was added dropwise at 0 °C. After stirring the reaction mixture for 15 min at 0 °C and an additional 4 h at room temperature the organic phase was removed under vacuum. The aqueous phase was diluted by addition of water (35 mL), washed with Et₂O (3 × 70 mL), acidified to pH 3 by adding 1 N HCl and extracted with EtOAc (4 × 70 mL). The combined organic phase obtained from the extractions was dried over sodium sulphate and evaporated under reduced pressure. Flash chromatography purification [eluent: DCM/MeOH, 9/1 (v/v) → DCM/MeOH, 4/1 (v/v)] yielded the platinum chelating amino acid **5** (1.25 g, 2.45 mmol, 65%) as a white solid. TLC [DCM/MeOH, 5/1 (v/v)]: *R_f* = 0.15. ¹H-NMR (300 MHz, DMSO-*d*₆): δ (ppm) = 7.88 (d, ³*J*_{H-H} = 6.72 Hz, 2-H, C4-Fmoc), 7.70 (m, 2-H, C1-Fmoc), 7.40 (t, ³*J*_{H-H} = 7.5 Hz, 2-H, C3-Fmoc), 7.33–7.30 (m, 2-H, C2-Fmoc), 5.95–5.87 (m, 1-H, CH-Alloc), 5.25 (d, ³*J*_{H-H} = 18.6 Hz, 1-H, =CH₂), 5.17–5.13 (m, 1-H, =CH₂), 4.50–4.48 (m, 2-H, CH₂-Alloc), 4.31–4.24 (m, 2-H, CH₂-Fmoc), 4.23–4.19 (m, 1-H, CH-Fmoc), 3.92–3.88 (m, 1-H, α-CH), 3.29 (t, ³*J*_{H-H} = 6.6 Hz, 2-H, CONCH₂), 2.83 (s_{br}, 3-H, CONCH₃), 2.44 (t, ³*J*_{H-H} = 6.6 Hz, 2-H, NCH₂), 2.33 (s_{br}, 2-H, δ-CH₂), 2.16 (s, 3-H, NCH₃), 1.74–1.68 (m, 1-H, β-CH₂), 1.62–1.56 (m, 1-H, β-CH₂), 1.49–1.41 (m, 2-H, γ-CH₂). ¹³C-NMR (125 MHz, DMSO-*d*₆): δ (ppm) = 174.2 (COOH), 155.8 (CO-Fmoc), 155.1 (CO-Alloc), 143.7 (C6-Fmoc), 140.7 (C5-Fmoc), 133.52 (CH=Alloc), 127.5 (C3-Fmoc), 127.0 (C2-Fmoc), 125.2 (C1-Fmoc), 120.0 (C4-Fmoc), 116.7 (=CH₂-Alloc), 65.5 (CH₂-Alloc), 65.0 (CH₂-Fmoc), 56.7 (δ-CH₂), 54.7 (NCH₂), 54.1 (α-CH), 46.7 (CH-Fmoc), 45.8 (CONCH₂), 41.5 (NCH₃), 33.9 (CONCH₃), 29.1 (β-CH₂), 23.0 (γ-CH₂). MS (ESI): *m/z* = 510.3 [M + H]⁺, 532.3 [M + Na]⁺, 548.2 [M + K]⁺, 1019.5 [2M + H]⁺. HRMS (ESI) = calculated for [C₂₈H₃₆N₃O₆]⁺ ([M + H]⁺) = 510.2599, found = 510.2601.

Synthesis of peptides 7a–c. The synthesis of the peptides started with NovaSyn® TGT resin (0.21 mmol per g resin loading density) preloaded with glycine. Standard Fmoc-based protocol on a scale of 0.1 mmol of resin was carried out. All amino acids were double coupled for 45 min at room temperature and for every coupling reaction the incoming amino acid (5 eq.) was used in combination with HATU (4.9 eq.), HOAt (5 eq.) and DIEA (5 eq.). Equivalents of Fmoc-Lys(Fmoc)-OH as well as that of the activators and the activator base for coupling the second and the third generation dendrimer were doubled and quadrupled, respectively. The Fmoc deprotection was performed using 20% piperidine in NMP for 10 min at room temperature. Cleavage of the peptides **7a–c** was done utilizing 30% HFIP in DCM for 45 min at room temperature. The crude peptide was precipitated in cold ether followed by cold centrifugation. The isolated residue was further purified by RP-HPLC and analyzed by mass spectrometry. **7a** Yield: 48%; HPLC (10–60% B in 30 min) *t_R* = 24.5 min. MS (ESI): *m/z* = 2040.3, [M + H]⁺, 1020.7 [M + 2H]²⁺, 680.8 [M + 3H]³⁺. HRMS (ESI) = calculated for [C₉₅H₁₇₇N₂₃O₂₅]²⁺ ([M + 2H]²⁺) = 1020.6652, found = 1020.6649. **7b** Yield: 53%; HPLC (10–60%

B in 30 min) *t_R* = 23.6 min. MS (ESI): *m/z* = 2040.4 [M + H]⁺, 1020.7 [M + 2H]²⁺, 680.8 [M + 3H]³⁺. HRMS (ESI) = calculated for [C₉₅H₁₇₈N₂₃O₂₅]³⁺ ([M + 3H]³⁺) = 680.7792, found = 680.7779. **7c** Yield: 58%; HPLC (10–60% B in 30 min) *t_R* = 24.7 min. MS (ESI): *m/z* = 2040.4 [M + H]⁺, 1020.7 [M + 2H]²⁺, 680.8 [M + 3H]³⁺, 510.8 [M + 4H]⁴⁺. HRMS (ESI) = calculated for [C₉₅H₁₇₈N₂₃O₂₅]³⁺ ([M + 3H]³⁺) = 680.7792, found = 680.7800.

Synthesis of peptides 8a–c. To a solution of the dendrimeric peptide **7a–c** in dry DMF (1 mL per 20 mg of dendrimer) DIC (4 eq.), NMM (5 eq.) and HOAt (3.95 eq.) were added under an inert atmosphere. The mixture was stirred for 10 min at room temperature followed by addition of the cyclic peptide **6** (0.5 eq.). After additional stirring of the reaction mixture for 48 h at room temperature the solvent was removed under vacuum and the residue was purified by RP-HPLC. **8a** Yield: 47%; HPLC (55–75% B' in 30 min) *t_R* = 20.3 min. MS (ESI): *m/z* = 1345.8 [M + 3H]³⁺, 1009.6 [M + 4H]⁴⁺, 807.9 [M + 5H]⁵⁺. HRMS (ESI) = calculated for [C₁₉₆H₃₂₆N₄₁O₄₇S]⁵⁺ ([M + 5H]⁵⁺) = 807.8821, found = 807.8820. **8b** Yield: 53%; HPLC (30–100% B' in 30 min) *t_R* = 22.4 min. MS (ESI): *m/z* = 1346.2 [M + 3H]³⁺, 1009.9 [M + 4H]⁴⁺, 808.1 [M + 5H]⁵⁺. HRMS (ESI) = calculated for [C₁₉₆H₃₂₆N₄₁O₄₇S]⁵⁺ ([M + 5H]⁵⁺) = 808.0826, found = 808.0829. **8c** Yield: 44%; HPLC (30–100% B' in 30 min) *t_R* = 25.1 min. MS (ESI): *m/z* = 2018.7 [M + 2H]²⁺, 1346.1 [M + 3H]³⁺, 1009.9 [M + 4H]⁴⁺, 808.1 [M + 5H]⁵⁺. HRMS (ESI) = calculated for [C₁₉₆H₃₂₅N₄₁O₄₇S]⁴⁺ ([M + 4H]⁴⁺) = 1009.8514, found = 1009.8531.

Synthesis of peptides 9a–c. To a solution of peptides **8a–c** in dry DMF (1 mL per 10 mg of peptide) Me₂NH.BH₃ (40 eq.) and Pd(PPh₃)₄ (0.1 eq.) were added under an inert atmosphere. After stirring the reaction mixture for 6 h at room temperature the solvent was removed and the residue was purified by RP-HPLC. **9a** Yield: 66%; HPLC (60–100% B in 30 min) *t_R* = 14.4 min. MS (ESI): *m/z* = 1976.7 [M + 2H]²⁺, 1318.1 [M + 3H]³⁺, 988.8 [M + 4H]⁴⁺, 791.3 [M + 5H]⁵⁺. HRMS (ESI) = calculated for [C₁₉₂H₃₂₀N₄₁O₄₅S]³⁺ ([M + 3H]³⁺) = 1318.1258, found = 1318.1269. **9b** Yield: 77%; HPLC (65–80% B in 30 min) *t_R* = 19.1 min. MS (ESI): *m/z* = 1318.1 [M + 3H]³⁺, 988.8 [M + 4H]⁴⁺, 791.3 [M + 5H]⁵⁺. HRMS (ESI) = calculated for [C₁₉₂H₃₂₁N₄₁O₄₅S]⁴⁺ ([M + 4H]⁴⁺) = 988.8462, found = 988.8483. **9c** Yield: 72%; HPLC (60–80% B in 30 min) *t_R* = 16.2 min. MS (ESI): *m/z* = 1318.1 [M + 3H]³⁺, 988.8 [M + 4H]⁴⁺, 791.3 [M + 5H]⁵⁺, 659.6 [M + 6H]⁶⁺. HRMS (ESI) = calculated for [C₁₉₂H₃₂₂N₄₁O₄₅S]⁵⁺ ([M + 5H]⁵⁺) = 791.2784, found = 791.2795.

Synthesis of peptides 10a–c. Peptides **9a–c** and potassium tetrachloroplatinate (30 eq.) were dissolved in DMF/H₂O (1 mL per 5 mg of peptide, 9/1 (v/v)). After stirring the reaction mixture for 48 h under exclusion of light at room temperature the solvent was removed under vacuum. The residue obtained was purified by RP-HPLC. **10a** Yield: 69%; HPLC (15–70% B in 30 min) *t_R* = 35.1 min. MS (ESI): *m/z* = 2109.6 [M + 2H]²⁺, 1406.8 [M + 3H]³⁺, 1055.6 [M + 4H]⁴⁺. HRMS (ESI) = calculated for [C₁₉₂H₃₂₁Cl₂N₄₁O₄₅SPT]⁴⁺ ([M + 4H]⁴⁺) = 1055.5717, found = 1055.5759. **10b** Yield: 62%; HPLC (15–75% B in 30 min) *t_R* = 35.2 min. MS (ESI): *m/z* = 1406.8 [M + 3H]³⁺, 1055.3 [M + 4H]⁴⁺,



845.5 $[M + 5H]^{5+}$. HRMS (ESI) = calculated for $[C_{192}H_{321}Cl_2N_{41}O_{45}PtS]^{4+}$ ($[M + 4H]^{4+}$) = 1055.3215, found = 1055.3273. **10c** Yield: 71%; HPLC (15–70% B in 30 min) t_R = 35.2 min. MS (ESI): m/z = 1406.8 $[M + 3H]^{3+}$, 1055.3 $[M + 4H]^{4+}$. HRMS (ESI) = calculated for $[C_{192}H_{320}Cl_2N_{41}O_{45}SPT]^{3+}$ ($[M + 3H]^{3+}$) = 1406.7595, found = 1406.7617.

Synthesis of peptides IHF-2/3/4. The peptides **10a–c** were dissolved in aqueous 95% TFA (1 mL for 10 mg of peptide) and the reaction mixture was stirred for 45 min at room temperature. Thereafter, the solvent was evaporated by drying with argon and the crude peptide was precipitated by pouring into cold ether. The residue obtained after cold centrifugation was purified by RP-HPLC. **IHF-2** Yield: 43%; HPLC (10–40% B in 30 min) t_R = 14.4 min. MS (ESI): m/z = 1527.3 $[M + 2H]^{2+}$, 1018.5 $[M + 3H]^{3+}$, 764.2 $[M + 4H]^{4+}$, 611.5 $[M + 5H]^{5+}$. HRMS (ESI) = calculated for $[C_{123}H_{227}Cl_2N_{41}O_{32}Pt]^{4+}$ ($[M + 4H]^{4+}$) = 764.1603, found = 764.1603. **IHF-3** Yield: 56%; HPLC (10–40% B in 30 min) t_R = 14.9, 15.5, 15.9 min. MS (ESI): m/z = 1528.3 $[M + 2H]^{2+}$, 1018.9 $[M + 3H]^{3+}$, 764.2 $[M + 4H]^{4+}$, 611.7 $[M + 5H]^{5+}$. HRMS (ESI) = calculated for $[C_{123}H_{225}Cl_2N_{41}O_{32}Pt]^{2+}$ ($[M + 2H]^{2+}$) = 1528.3140, found = 1528.3128. **IHF-4** Yield: 51%; HPLC (10–40% B in 30 min) t_R = 15.0, 15.7, 16.2 min. MS (ESI): m/z = 1019.2 $[M + 3H]^{3+}$, 764.4 $[M + 4H]^{4+}$, 611.7 $[M + 5H]^{5+}$, 509.9 $[M + 6H]^{6+}$, 437.2 $[M + 7H]^{7+}$. HRMS (ESI) = calculated for $[C_{123}H_{226}Cl_2N_{41}O_{32}Pt]^{3+}$ ($[M + 3H]^{3+}$) = 1019.2118, found = 1019.2139.

Thermal melting analysis. A 34-mer DNA sequence containing a GG-site within 5'-TCGTTGCAACAAATTGATAGGCAATGCT-TTTTGA-3' was mixed in a 1:1 ratio with its complementary strand 5'-TAAAAAGCATTGCCTATCAATTTGTTGCAACGA-3' in 10 mM phosphate buffer (Na_2HPO_4/NaH_2PO_4 , pH = 5.8). The two strands were annealed by heating at 95 °C for 5 min followed by slow cooling to room temperature for 30 min to form duplex **D1**. Thereafter, the peptides were mixed with the duplex **D1** such that the final concentration of the peptide was 5 μ M and that of the duplex was 1 μ M in 10 mM phosphate buffer (Na_2HPO_4/NaH_2PO_4 , pH = 5.8). The peptides were pre-incubated for 17 h at 37 °C with the duplex **D1** prior to measurement. All experiments were performed in at least as triplicates on independent occasions in 1 cm quartz cuvettes. A Cary 100 UV/Vis spectrophotometer (Varian) equipped with a multiple cell holder and a Peltier temperature controller was utilized to measure the absorbance *versus* temperature profiles at 250 nm. The data points were taken after every 0.5 °C at a heating/cooling rate of 0.7 °C min⁻¹ during the cycles. The T_m values are given as the calculated maximum of the first derivative of the curves.

Agarose gel electrophoresis. A gel mobility shift assay to study the interactions of the peptides with plasmid DNA (pUC18, purified by use of a midi-prep kit from Sigma-Aldrich) was performed on non-denaturing agarose gels (1% agarose, 1 \times TAE (40 mM Tris, 20 mM acetic acid, 1 mM EDTA, pH = 8)). The gels were run in 1 \times TAE buffer at a constant voltage (6 V cm⁻¹) for 1.5 h. The concentration of the plasmid DNA was determined by Nanodrop ND-2000c spectrometer in ng μ L⁻¹,

which was converted to nmol (of nucleobase) per μ L by division with 324 (average weight of DNA nucleotide). The final concentration of the DNA in each reaction was maintained as 0.2 mM nucleobases whereas the concentration of the peptides was varied from r_f values 0 to 0.15; r_f is defined as $C_{peptide}/C_{nucleotide}$. Prior to electrophoresis the peptides were incubated with the plasmid DNA for 2 h at 37 °C in 10 mM phosphate buffer (Na_2HPO_4/NaH_2PO_4 , pH = 5.8) and the reactions were quenched by addition of 2 μ L of the loading dye (2.3 M urea, 1 \times TBE, 66% (v/v) formamide, 0.05% (w/v) bromophenol blue, 0.05% (w/v) xylene cyanol, 500 mM NaCl). After the electrophoresis the gel was stained in a solution of GelStar™ dye (5 μ L in 50 mL of 1 \times TAE buffer containing 3 M NaCl) and imaged by utilizing UV transillumination.

Polyacrylamide gel electrophoresis. Native and denaturing gel electrophoresis (0.4 mm thick, 20 \times 45 cm, 20% acrylamide, 7 M urea (only for denaturing gels), 1 \times TBE (89 mM Tris, 89 mM boric acid, 2 mM EDTA, pH = 8) were performed to investigate the interactions of the IHF mimicking peptides with a 34-bp consensus sequence containing (5'-TCGTTGCAACAAATTGATA-GGCAATGATTTTTTGA-3') or excluding (5'-TCGTTGCAACAAATTGA-TAAGCAATGATTTTTTGA-3') the preferred platination site (GG site). The gels were run in 1 \times TBE buffer at a constant current of 20 W for 1.5–2 h. The DNA oligomers labeled with 6-FAM (6-carboxyfluorescein) at the 5'-end for visualization were annealed with their corresponding complementary non-labeled sequences. Prior to electrophoresis the peptides were incubated with the duplex DNA in phosphate buffer (10 mM Na_2HPO_4/NaH_2PO_4 , 100 mM $NaClO_4$, pH = 5.8) wherein the concentration of DNA (C_{DNA}) = 0.5 μ M and the concentration of the peptide ($C_{peptide}$) = 10 μ M. The reaction was quenched by addition of 2 μ L of the marker 6 \times TriTrack loading dye (10 mM Tris, 60 mM EDTA, 0.03% bromophenol blue, 0.03% xylene cyanol FF, 0.15% orange G, 60% glycerol, pH = 7.6) from Fermentas. The fluorescence gels were imaged on a Typhoon 9400 Variable Mode Gel Imager from Amersham Biosciences (GE Healthcare) by scanning under the blue laser module and quantified by the ImageQuant software.

Conclusions

In this work, we have presented a combinatorial chemistry approach to design peptide based platinum metal complexes mimicking the sequence specific DNA binding protein, IHF. The synthesis of platinum complex/peptide chimera was achieved by tethering a platinum chelating unit to a model peptide mimicking IHF. Gel mobility shift assays indicate the importance of synergistic interactions resulting from the minor groove binding cyclic peptide, the positively charged lysine dendrimer and the platinum unit, combined together for efficient DNA targeting. However, establishing elements of sequence specific recognition is desirable and can be achieved by further optimizing the design of biomimetic model peptides. Utilizing such DNA targeting peptide designs offers the possibility to develop a novel library of platinum based hybrid



chemotherapeutic agents possessing enhanced DNA interaction properties.

Acknowledgements

Generous support from Deutsche Forschungsgemeinschaft (DFG, IRTG 1422) is gratefully acknowledged. Furthermore, we are also grateful for financial support from the Swedish Cancer Foundation, Swedish Research Council and FLÄK (Research School in Pharmaceutical Science, Lund University).

References

- S. E. Sherman, D. Gibson, A. H.-J. Wang and S. J. Lippard, *Science*, 1985, **230**, 412.
- A. Eastman, *Biochemistry*, 1986, **13**, 3912.
- J. Reedjik, *Pure Appl. Chem.*, 1987, **59**, 181.
- P. M. Takahara, A. C. Rosenzweig, C. A. Frederick and S. J. Lippard, *Nature*, 1995, **377**, 649.
- L. Kelland, *Nat. Rev. Cancer*, 2007, **7**, 573.
- M. H. Werner, J. R. Huth, A. M. Gronenborn and G. M. Clore, *Cell*, 1995, **81**, 705.
- C. S. Chow, C. M. Barnes and S. J. Lippard, *Biochemistry*, 1995, **34**, 2956.
- U. M. Ohndorf, M. A. Rould, Q. He, C. O. Pabo and S. J. Lippard, *Nature*, 1999, **399**, 708.
- D. E. Fisher, *Cell*, 1994, **78**, 539.
- J. C. Huang, D. B. Zamble, J. T. Reardon, S. J. Lippard and A. Sancar, *Proc. Natl. Acad. Sci. U. S. A.*, 1994, **91**, 10394.
- J. Zlatanova, J. Yaneva and S. H. Leuba, *FASEB J.*, 1998, **12**, 791.
- M. Kartalou and J. M. Essigmann, *Mutat. Res.*, 2001, **478**, 1.
- A. Mandic, J. Hansson, S. Lider and M. C. Shoshan, *J. Biol. Chem.*, 2003, **278**, 9100.
- F. Yu, J. Megyesi and P. M. Price, *Am. J. Physiol.*, 2008, **295**, F44.
- T. Gianferrara, I. Bratsos and E. Alessio, *Dalton Trans.*, 2009, 7588.
- S. Dasari and P. B. Tchounwou, *Eur. J. Pharmacol.*, 2014, **740**, 364.
- S. L. Bruhn, J. H. Toney and S. J. Lippard, *Prog. Inorg. Chem.*, 1990, **38**, 477.
- K. Wang, J. F. Lu and R. C. Li, *Coord. Chem. Rev.*, 1996, **151**, 53.
- E. R. Jamieson and S. J. Lippard, *Chem. Rev.*, 1999, **99**, 2467.
- P. Jordan and M. Carmo-Fonseca, *Cell. Mol. Life Sci.*, 2000, **57**, 1229.
- S. R. McWhinney, R. M. Goldberg and H. L. McLeod, *Mol. Cancer Ther.*, 2009, **8**, 10.
- I. Arany and R. L. Safirstein, *Semin. Nephrol.*, 2003, **23**, 460.
- J. T. Hartmann, L. M. Fels, S. Knop, H. Stolt, L. Kanz and C. Bokemeyer, *Invest. New Drugs*, 2000, **18**, 281.
- J. T. Hartmann and H. P. Lipp, *Expert Opin. Pharmacother.*, 2003, **4**, 889.
- G. Giaccone, *Drugs*, 2000, **59**, 9.
- M. A. Fuertes, C. Alonso and J. M. Perez, *Chem. Rev.*, 2003, **103**, 645.
- R. Hamzavi, T. Happ, K. Weitershaus and N. Metzler-Nolte, *J. Organomet. Chem.*, 2004, **689**, 4745.
- F. Noor, A. Wüstholtz, R. Kinscherf and N. Metzler-Nolte, *Angew. Chem., Int. Ed.*, 2005, **45**, 2429.
- G. Dirscherl and B. König, *Eur. J. Org. Chem.*, 2008, 597.
- A. C. Komor and J. K. Barton, *Chem. Commun.*, 2013, **45**, 3617.
- C. Borghouts, C. Kunz and B. Groner, *J. Pept. Sci.*, 2005, **11**, 713.
- L. Crespo, G. Sanclimens, M. Pons, E. Giralt, M. Royo and F. Albericio, *Chem. Rev.*, 2005, **105**, 1663.
- H. Cai, M.-S. Chen, Z.-Y. Sun, Y.-F. Zhao, H. Kunz and Y.-M. Li, *Angew. Chem., Int. Ed.*, 2013, **52**, 6106.
- M. S. Damian, H. K. Hedman, S. K. C. Elmroth and U. Diederichsen, *Eur. J. Org. Chem.*, 2010, 6161.
- S. Van Zutphen and J. Reedjik, *Coord. Chem. Rev.*, 2005, **249**, 2845.
- N. Goosen and P. Van de Putte, *Mol. Microbiol.*, 1995, **16**, 1.
- N. Goosen and P. Van de Putte, *Mol. Microbiol.*, 1996, **6**, 2557.
- D. I. Friedman, *Cell*, 1988, **55**, 545.
- H. Nash, in *Regulation of Gene Expression in Escherichia Coli*, eds. E. C. C. Lin and A. S. Lynch, R. G. Landes Company, Austin, Texas, 1996, p. 149.
- P. A. Rice, S.-W. Yang, K. Mizuuchi and H. A. Nash, *Cell*, 1996, **87**, 1295.
- E. K. Liebler and U. Diederichsen, *Org. Lett.*, 2004, **6**, 2893.
- S. Scholz, E. K. Liebler, B. Eickmann, H.-J. Fritz and U. Diederichsen, *Amino Acids*, 2012, **43**, 289.
- U. Diederichsen, D. Weicherding and N. Diezemann, *Org. Biomol. Chem.*, 2005, **3**, 1058.
- D. Fernández-Fornier, G. Casala, E. Navarro, H. Ryder and F. Albericio, *Tetrahedron Lett.*, 2001, **42**, 4471.
- S. F. Bellon, J. H. Coleman and S. J. Lippard, *Biochemistry*, 1991, **30**, 8026.
- G. L. Cohen, W. R. Bauer, J. K. Barton and S. J. Lippard, *Science*, 1979, **203**, 1014.
- L. S. Lerman and H. L. Frisch, *Biopolymers*, 1982, **21**, 995.
- M. Leng, *Biophys. Chem.*, 1990, **35**, 155.
- S. F. Bellon and S. J. Lippard, *Biophys. Chem.*, 1990, **35**, 179.
- C. Hofr and V. Brabec, *Biopolymers*, 2005, **77**, 222.
- N. Poklar, D. S. Pitch, S. J. Lippard, E. A. Redding, S. U. Dunham and K. J. Breslauer, *Proc. Natl. Acad. Sci. U. S. A.*, 1996, **93**, 7606.
- M. C. Olmsted, J. P. Bond, C. F. Anderson and M. T. Record, *Biophys. J.*, 1995, **68**, 634.
- R. M. Hughes, M. L. Benshoff and M. L. Waters, *Chem. – Eur. J.*, 2007, **13**, 5753.

